

Sub-surface signatures of the Atlantic Multidecadal Oscillation

L. M. Frankcombe,¹ H. A. Dijkstra,¹ and A. von der Heydt¹

Received 11 June 2008; revised 22 August 2008; accepted 27 August 2008; published 2 October 2008.

[1] Sub-surface signatures of the Atlantic Multidecadal Oscillation (AMO) are identified using expendable bathythermograph (XBT) measurements of temperature from the surface down to a depth of 400 m. Basin averaged temperature anomalies in the North Atlantic at different depths display multidecadal variability with a phase shift between temperature anomalies at the surface and at depth. Westward propagation of temperature anomalies is observable at depth and there is a lag correlation between east-west and north-south temperature gradients, with the east-west temperature gradient leading. These sub-surface characteristics of the AMO agree with those expected from the noise-driven internal ocean mode view of the AMO, as derived from a hierarchy of ocean-atmosphere models. **Citation:** Frankcombe, L. M., H. A. Dijkstra, and A. von der Heydt (2008), Sub-surface signatures of the Atlantic Multidecadal Oscillation, *Geophys. Res. Lett.*, 35, L19602, doi:10.1029/2008GL034989.

1. Introduction

[2] It is now well established that North Atlantic sea surface temperature (SST) displays variability on multidecadal time scales [Kushnir, 1994; Enfield *et al.*, 2001], a phenomenon usually referred to as the Atlantic Multidecadal Oscillation (AMO) [Kerr, 2000]. An AMO index, defined by Enfield *et al.* [2001] as a ten year running mean of SST anomalies averaged over the Atlantic basin north of the equator, shows that North Atlantic SSTs were cooler than average in the periods 1900–1920 and 1970–1990 with an intervening warmer period during 1940–1960.

[3] Multidecadal to centennial SST variability has been simulated in various coupled general circulation models and several different mechanisms have been proposed. While there is a general consensus that the Atlantic Meridional Overturning Circulation (MOC) is involved, some researchers attribute a central role to the tropics [Vellinga and Wu, 2004; Knight *et al.*, 2005], some stress the importance of the Arctic ocean [Jungclauss *et al.*, 2005], while others find that only North Atlantic processes are essential [Delworth *et al.*, 1993; Dong and Sutton, 2005].

[4] Another approach to understanding AMO variability uses a hierarchy of ocean and coupled ocean-atmosphere models and follows the characteristics of the multidecadal variability through this model hierarchy [Huck *et al.*, 1999; *te Raa and Dijkstra*, 2002; *Dijkstra et al.*, 2008]. Uncoupled ocean models provide a detailed picture of how multi-

decadal variability arises from the geostrophic and hydrostatic response to westward propagating temperature (or density) anomalies, with an out of phase response of the MOC and the zonal overturning [*te Raa and Dijkstra*, 2002]. More sophisticated models have clarified the role of the atmosphere: low-frequency components of atmospheric variability are important to excite the multidecadal variability in the ocean [Delworth and Greatbatch, 2000; Frankcombe *et al.*, 2008].

[5] The noise-driven internal mode view of the AMO which arises from this hierarchical modeling approach has two central elements: the westward propagation of temperature anomalies and a phase difference between east-west and north-south temperature differences. The westward propagation is associated with so-called thermal Rossby modes and hence is affected by the background time mean ocean state. Ocean-only models show that the propagation is clearest below the ocean surface because of the smaller background zonal velocities and the decreased influence of noisy surface forcing.

[6] While the characteristics of the AMO in terms of SST variability are more or less well established, basin wide variability in sub-surface layers has not been investigated due to the scarcity of data and the short length of the available timeseries compared to the estimated period of the variability. Motivated by the view of the AMO obtained from the model hierarchy we investigate westward propagation and lateral temperature differences in the sub-surface North Atlantic using XBT data.

[7] The present study uses ocean temperatures from the Joint Environment Data Analysis (JEDA) Center (<http://jedac.ucsd.edu/index.html>). This data set consists of monthly mean ocean temperatures from January 1955 to December 2003 (588 months) in 11 layers between the sea surface and 400 m depth. The data is interpolated on to a 5° longitude by 2° latitude grid between 60°N and 60°S. Anomalies are calculated with respect to the time mean over the whole time period. No trends have been removed due to the difficulty of separating the anthropogenic warming trend from natural variability.

2. Sub-surface AMO Indices

[8] Following Enfield *et al.* [2001] we define subsurface AMO indices as the ten year running mean of North Atlantic temperature anomalies in each layer over the region 0–60°N, 85°W–5°E. The results are shown in Figure 1a. It is apparent that there is a phase shift between the surface and the lower layers, particularly in the earlier part of the record. While the basin-averaged SST was cooling over the period 1960–1972 for example, by 1967 the temperature at 400 m was already increasing. After 1990 the sub-surface and surface signal are more in

¹Institute for Marine and Atmospheric Research Utrecht, Department of Physics and Astronomy, Utrecht University, Utrecht, Netherlands.

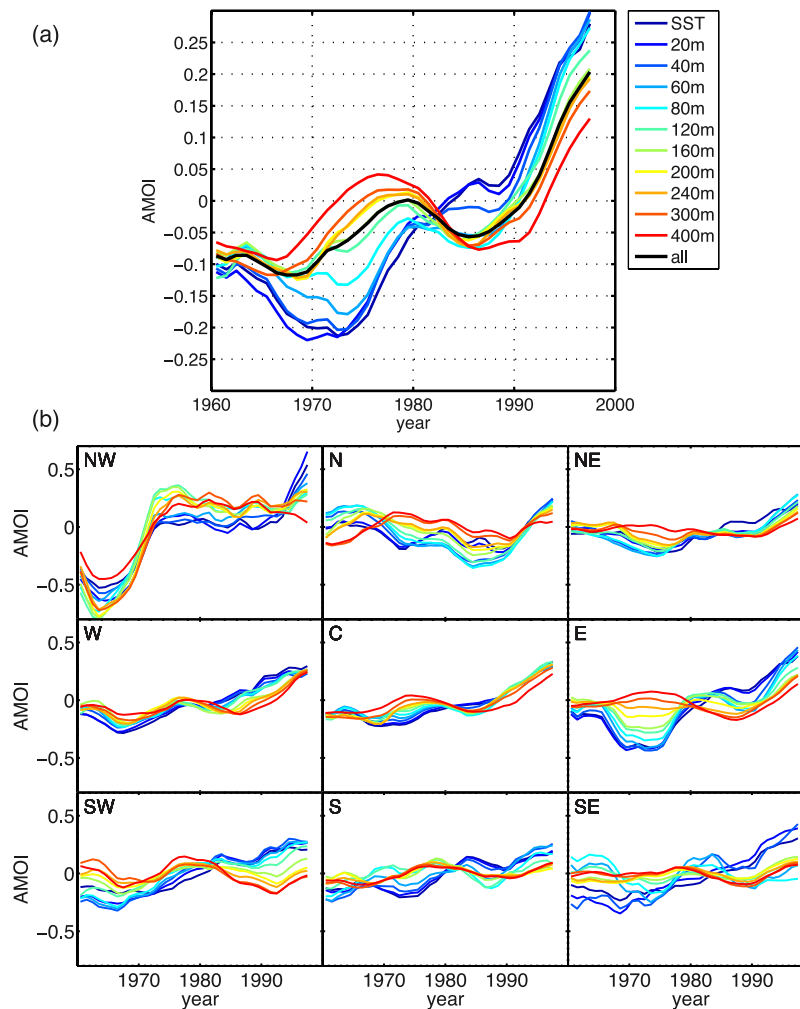


Figure 1. (a) Temperature anomalies at different levels averaged over the North Atlantic basin with a ten year running mean. The black line shows the basin averaged temperature over all layers from the surface to 400 m. Note that no trends have been removed from this data. (b) Similar indices calculated over sub-regions within the North Atlantic. Colours are as in a and the regions are the north-west (NW; top left), central north (N; top centre), north-east (NE; top right) and so on.

phase, consistent with the warming trend in the upper-ocean heat content [Levitus *et al.*, 2000] attributed to anthropogenic climate change.

[9] We examine the sub-surface spatial pattern of the AMO by dividing the basin into nine sub-regions (north west, central north, north east, central west, center, etc.) and calculating temperature anomalies at each level within each region. The results are shown in Figure 1b. The largest temperature anomalies are seen in the north-west of the basin. The anomalies in the west, particularly the central and north-western regions, are more uniform with depth while the phase difference between different layers seen in the overall AMO index (Figure 1a) is more apparent in the central and eastern parts of the basin.

[10] Another interesting feature which can be seen in Figure 1b is the warming after 1990. In the north of the basin the warming starts in all layers at the same time while in the south there is a delay between the onset of warming in the upper and lower layers. It is very likely that this is

related to the presence of the sinking region in the north of the basin [Levitus *et al.*, 2000].

3. Sub-surface Propagation Characteristics

[11] Following Kushnir [1994] we calculate the difference between two warm and two cool periods to illustrate the patterns of warming and cooling of the upper and lower layers at different times. First we use the periods 1970–1972 (upper layers anomalously cool) and 1959–1961 (upper layers anomalously warm). Figure 2 shows the spatial pattern of the difference between these two periods at two different depths, the upper (0–80 m, Figure 2a) and lower (300–400 m, Figure 2b) layers.

[12] In Figure 2a the temperature anomalies are positive over most of the basin, with a particularly strong anomaly in the east. A strong negative anomaly, the remains of the previous cool phase, appears in the north west. This cool anomaly can also be seen at depth in Figure 2b where much

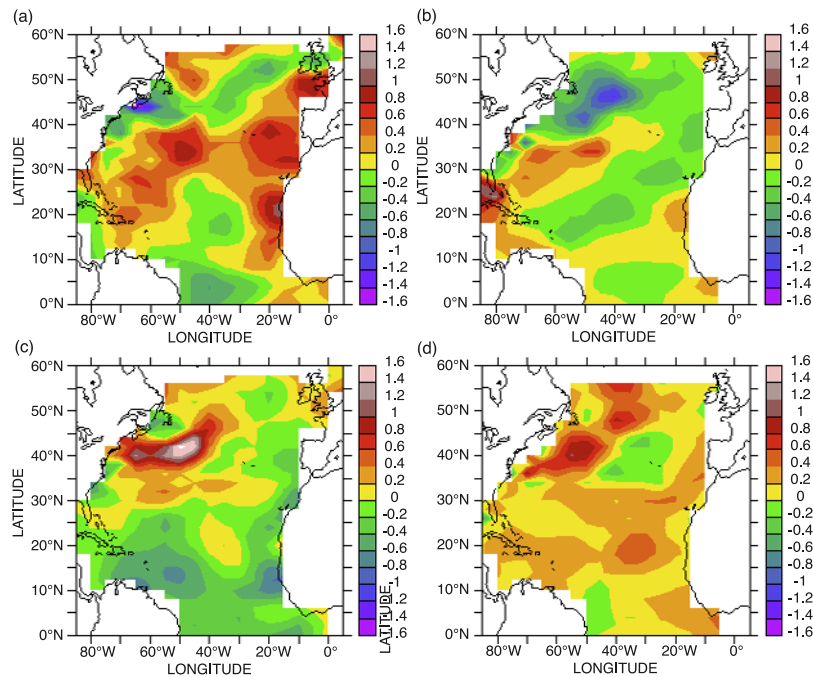


Figure 2. Surface and sub-surface patterns. The temperature during the period 1970–1972 (cool in upper layers) has been subtracted from the temperature during the period 1959–1961 (warm in upper layers) for two different depths, (a) the upper (0–80 m) and (b) lower (300–400 m) layers. (c and d) As for Figures 2a and 2b but for the period 1986–1988 (cool in lower layers) subtracted from the period 1975–1977 (warm in lower layers).

of the basin is covered by negative temperature anomalies. This is consistent with the idea that temperature anomalies are more uniform with depth in the western part of the basin.

[13] Similar figures are shown using the periods 1986–1988 (lower layers anomalously cool) and 1975–1977 (lower layers anomalously warm; Figures 2c and 2d). These patterns are almost the opposite of those in Figures 2a and 2b. At the surface a warm anomaly covers most of the north while a cold anomaly is just beginning to develop in the south. In the deeper layers a warm anomaly covers most of the basin. The intense warm anomaly seen at the surface in the north west is also apparent at depth.

[14] Basin-wide westward propagation of temperature anomalies is an important feature of the AMO as found in simpler models [*te Raa and Dijkstra, 2002*]. A Hovmöller diagram of temperature anomalies averaged over 10° – 60° N at a depth of 300–400 m is shown in Figure 3a. Since the anomalies are advected northwards by the mean circulation as they travel west across the basin it is necessary to average over a range of latitudes to see the full propagation. Averaging over the entire basin highlights the basin-wide nature of the phenomenon. A cold (warm) anomaly in the eastern part of the basin after 1960 (1970) travelled westwards, reaching the western part of the basin after 1970 (1980). A second cold anomaly developed in the east after 1980, however by this time the warming trend begins to dominate the signal and propagation is less clear. The westward propagation is most clearly seen at a depth of 300–400 m, the lowest levels included in the data set. It is also most clearly seen in boreal summer (JJA), when the shallower mixed layer keeps noise confined to the surface,

and between the latitudes 20° – 30° N (south of the Gulf Stream; not shown). Eastward propagation of anomalies is observed in the upper layers at the latitude of the Gulf Stream, in agreement with *Hansen and Bezdek [1996]* and *Sutton and Allen [1997]*.

[15] A Hovmöller plot of heat content from the surface to a depth of 400 m is shown in Figure 3b. The timing of the warm and cool anomalies agrees with the temperature anomalies although westward propagation is not seen in the heat content due to the strong eastward flow of the Gulf Stream and North Atlantic Drift at the surface. If the averaging is restricted to 10° – 30° N then westward propagation becomes visible at the beginning of the record (not shown). Figure 3b can be used to interpret the pattern of heat storage found by *Levitus et al. [2000, Figure 3a]* between the period 1970–1974 and 1988–1992. The change in heat content during this time can be largely attributed to the AMO (although it also includes the signal of anthropogenic warming) and the pattern of the anomalies is related to the temperature anomalies in Figure 2.

[16] Another feature of the AMO central to the noise driven internal mode view is a phase difference between the zonally averaged north-south surface temperature difference T_{N-S} and the meridionally averaged east-west surface temperature difference T_{E-W} , with T_{E-W} leading by about a quarter of a period [*te Raa and Dijkstra, 2002*]. Temperature anomalies in the east, west, north and south of the basin were calculated using the masks shown in Figure 4a. The lag correlation of five year running means of T_{N-S} and T_{E-W} is plotted in Figure 4b for temperatures measured at the surface (red) and averaged from the surface to a depth of 400 m (blue). Significant correlations occur when T_{E-W}

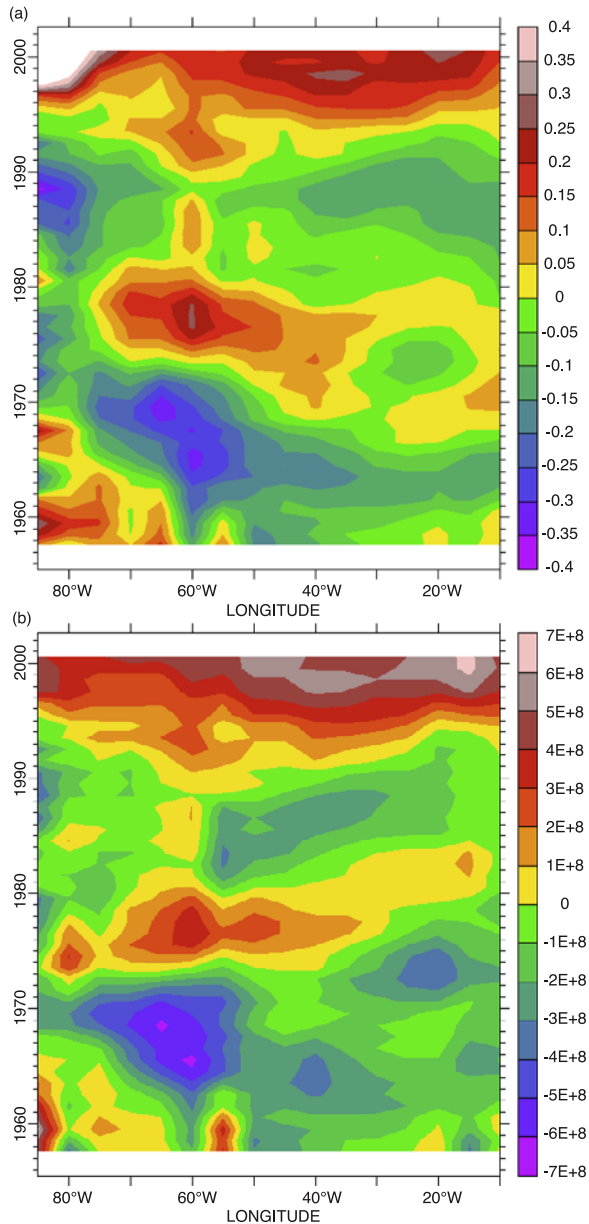


Figure 3. Hovmöller plot averaged over 10° – 60° N across the North Atlantic of (a) temperature anomalies at a depth of 300–400 m and (b) heat content from the surface to 400 m. Five year running means have been applied.

leads T_{N-S} , with a peak around 8 years at the surface and around 5 years for the depth averaged temperatures. The positive correlation at positive lag in Figure 4b agrees qualitatively with the propagation mechanism suggested by *te Raa and Dijkstra* [2002] which, given the quarter period lead in this mechanism, would suggest a period of 20 to 32 years. This agrees with the number of anomalies seen in Figure 3 and is also consistent with the results of a number of GCMs [e.g., *Dong and Sutton*, 2005].

[17] On the other hand, AMO indices calculated from longer observational timeseries of SST [*Delworth and Mann*, 2000; *Enfield et al.*, 2001] estimate a considerably longer period of 50–70 years. Hence modulation of longer time scale SST variability is likely to be involved. The short

length of the timeseries used here does not allow us to calculate periods with any certainty.

4. Discussion

[18] We have investigated long-term variability in XBT data down to 400 m for the North Atlantic over the period 1955–2003. Although there may be a positive temperature bias of the XBT data with respect to CTD data [*Gouretski and Koltermann*, 2007], this should not affect the phase difference between the surface and sub-surface temperature as found here over the period 1960–1990. After 1990 the temperature signal of the upper 400 m is in phase and is most likely the global warming signal as determined from heat content studies [e.g., *Levitus et al.*, 2000].

[19] As expected from the mechanism of the AMO found in ocean-only models [*Frankcombe et al.*, 2008], we find westward propagation of sub-surface temperature anomalies and a phase difference between north-south and east-west temperature differences. This mechanism can be used to explain several features of the data. Anomalies develop at the surface close to the eastern boundary of the basin (as seen in Figures 2a and 2c) and travel north-westwards across the basin. At the western boundary the temperature

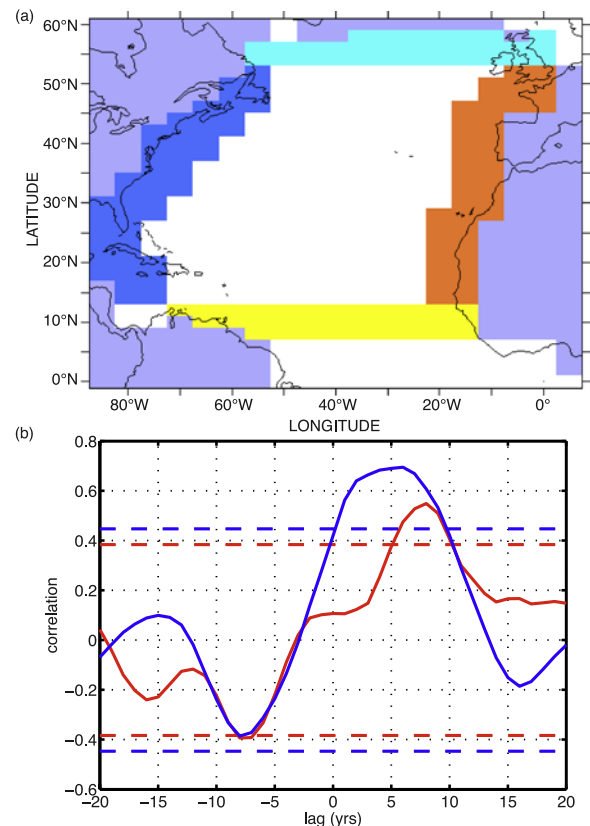


Figure 4. (a) The masks used to calculate the east-west and north-south temperature differences. Purple indicates land or areas with no data and the masks used are shown in blue (T_W), orange (T_E), yellow (T_S) and cyan (T_N). (b) Lag correlation between T_{N-S} and T_{E-W} at the surface (red) and averaged from the surface to 400 m (blue), with positive lags indicating that T_{E-W} leads. Dashed lines are 95% significance levels.

anomalies extend to their greatest depth. Figures 2b and 2d indeed have their largest anomalies in this part of the basin. This is supported by Figure 1b showing that in the western part of the basin the phase difference between surface and depth is small and in the north west the anomalies become uniform with depth. This is most likely related to the poleward deepening of the mixed layer. The phase difference between surface and depth was also observed by Molinari *et al.* [1997] in XBT data in the midlatitude western North Atlantic.

[20] The westward propagation also becomes clear by comparing the AMO index in the north west of the basin (top left box in Figure 1b) to the AMO index over the whole basin (Figure 1a): In the early 1960s, while SSTs over the basin as a whole were cooling, temperatures in the north west were just beginning to warm. This is due to the temperature anomaly from the previous phase of the oscillation remaining in the northern part of the basin while the next temperature anomaly is spreading (center right in Figure 1b). The newly developing warm anomaly (Figure 2b) is appearing at depth while the previous cool anomaly is advected to the north.

[21] As with most studies of multidecadal variability, the data record is too short to be able to make a strong statement on the periodicity of the AMO. The main point here is that the sub-surface phase lag, westward propagation and the lag between meridional and zonal temperature gradients that are predicted by the noise-driven internal ocean mode hypothesis (as proposed by Dijkstra *et al.* [2008]) as signatures of the AMO are all seen in the XBT data.

[22] **Acknowledgments.** We thank Molly Baringer (NOAA, Miami) and Amy Clement (RSMAS, Miami) for suggesting an analysis of the XBT data. AvdH acknowledges personal support through a VENI grant by the Netherlands Organisation for Scientific Research (NWO).

References

- Delworth, T. L., and R. J. Greatbatch (2000), Multidecadal thermohaline circulation variability driven by atmospheric surface flux forcing, *J. Clim.*, *13*, 1481–1495.
- Delworth, T. L., and M. E. Mann (2000), Observed and simulated multidecadal variability in the Northern Hemisphere, *Clim. Dyn.*, *16*, 661–676.
- Delworth, T. L., S. Manabe, and R. J. Stouffer (1993), Interdecadal variations of the thermohaline circulation in a coupled ocean-atmosphere model, *J. Clim.*, *6*, 1993–2011.
- Dijkstra, H. A., L. M. Frankcombe, and A. von der Heydt (2008), A stochastic dynamical systems view of the Atlantic Multidecadal Oscillation, *Philos. Trans. R. Soc.*, *366*, 2545–2560.
- Dong, B., and R. T. Sutton (2005), Mechanism of interdecadal thermohaline circulation variability in a coupled ocean-atmosphere GCM, *J. Clim.*, *18*, 1117–1135.
- Enfield, D. B., A. M. Mestas-Nuñez, and P. J. Trimble (2001), The Atlantic multidecadal oscillation and its relation to rainfall and river flows in the continental U.S., *Geophys. Res. Lett.*, *28*(10), 2077–2080.
- Frankcombe, L. M., H. A. Dijkstra, and A. von der Heydt (2008), Noise induced multidecadal variability in the North Atlantic: Excitation of normal modes, *J. Phys. Oceanogr.*, in press.
- Gouretski, V., and K. P. Koltermann (2007), How much is the ocean really warming?, *Geophys. Res. Lett.*, *34*, L01610, doi:10.1029/2006GL027834.
- Hansen, D. V., and H. F. Bezdek (1996), On the nature of decadal anomalies in North Atlantic sea surface temperature, *J. Geophys. Res.*, *101*(C4), 8749–8758.
- Huck, T., A. Colin de Verdière, and A. J. Weaver (1999), Interdecadal variability of the thermohaline circulation in box-ocean models forced by fixed surface fluxes, *J. Phys. Oceanogr.*, *29*, 865–892.
- Jungclaus, J. H., H. Haak, M. Latif, and U. Mikolajewicz (2005), Arctic–North Atlantic interactions and multidecadal variability of the meridional overturning circulation, *J. Clim.*, *18*, 4013–4031.
- Kerr, R. A. (2000), A North Atlantic climate pacemaker for the centuries, *Science*, *288*, 1984–1986.
- Knight, J. R., R. J. Allan, C. K. Folland, M. Vellinga, and M. E. Mann (2005), A signature of persistent natural thermohaline circulation cycles in observed climate, *Geophys. Res. Lett.*, *32*, L20708, doi:10.1029/2005GL024233.
- Kushnir, Y. (1994), Interdecadal variations in North Atlantic sea surface temperature and associated atmospheric conditions, *J. Clim.*, *7*, 141–157.
- Levitus, S., J. I. Antonov, T. P. Boyer, and C. Stephens (2000), Warming of the world ocean, *Science*, *287*, 2225–2229.
- Molinari, R. L., D. A. Mayer, J. F. Festa, and H. F. Bezdek (1997), Multi-year variability in the near-surface temperature structure of the midlatitude western North Atlantic Ocean, *J. Geophys. Res.*, *102*(C2), 3267–3278.
- te Raa, L. A., and H. A. Dijkstra (2002), Instability of the thermohaline ocean circulation on interdecadal timescales, *J. Phys. Oceanogr.*, *32*, 138–160.
- Sutton, R. T., and M. R. Allen (1997), Decadal predictability of North Atlantic sea surface temperature and climate, *Nature*, *388*, 563–567.
- Vellinga, M., and P. Wu (2004), Low-latitude freshwater influence on centennial variability of the Atlantic Thermohaline Circulation, *J. Clim.*, *17*, 4498–4511.
- H. A. Dijkstra, L. Frankcombe, and A. von der Heydt, Institute for Marine and Atmospheric Research Utrecht, Department of Physics and Astronomy, Utrecht University, Princetonplein 5, NL-3584 CC, Utrecht, Netherlands. (l.m.frankcombe@uu.nl)